Lecture 6

Jarle Brinchmann

11/03/2014

1 Introduction

Last week we looked first at how perturbations, and thus the correlation function and power spectrum, of dark matter in redshift space compare to those in real space. We found that on large scales, while the perturbations are in the linear regime, perturbations are boosted relative to real space through

$$\delta_k^{(s)} = \left(1 + f(\Omega_m)\mu^2\right)\delta_k, \tag{1}$$

where μ is the cosine of the angle between line of sight and the peculiar velocity. This boosting along the line of sight is often called the Kaiser effect and results from the fact that there is a mean infall of material towards the centres of perturbations relative to Hubble flow. On smaller scales we argued that peculiar velocities that result from virialisation will lead to elongation of structures along the line of sight in redshift space.

We then looked at the Press-Schechter mass function. To derive this we focused on the linear perturbation spectrum and based on the spherical collapse model we defined the criterion for collapse at time t is that

$$\delta^{\rm lin} > \delta_c(t) = \frac{\delta_c}{D(t)}, \tag{2}$$

where $\delta_c = 1.69$ is the extrapolated linear overdensity that a spherical top-hat perturbation would have when the real perturbation would have collapsed. The $D(t)$ is the growth function of the perturbations.

Together with the fact that the linear density perturbation field is Gaussian, this led to the Press-Schechter mass function:

$$\begin{aligned} n(M,t)dM &= \frac{\bar\rho}{M}\frac{\partial F(>M)}{\partial M}dM \\ &= \sqrt{\frac{2}{\pi}}\frac{\bar\rho}{M^2}\frac{\delta_c(t)}{\sigma(M)}e^{-\delta_c^2(t)/2\sigma^2(M)}\left|\frac{d\ln\sigma(M)}{d\ln M}\right|dM. \end{aligned} \tag{3}$$

Here $\sigma(M)$ is the variance of the density field on the scale M and $\bar\rho$ is the background density. Note that all of these quantities are evaluated at the present day with the exception of $\delta_c(t)$.

When we compared the PS mass function to a typical luminosity or mass function, we found that it has an excess of low and high mass halos relative to the stellar mass function.

2 The extended Press-Schechter formalism

This is not often discussed in detail in textbooks. There is a good discussion in section 7.2 and 7.3 in MvdBW and in section 17.2 of Peacock and these two sources form the basis of my exposition.

We will now return to the Press-Schechter formalism and discuss what is known as the *extended* Press-Schechter formalism, often shortened to EPS. To get a good understanding of this we start by re-deriving the PS mass function from this new formalism.

But before we get to this, it might be worth taking a philosophical view of why we will do what we will do. In the discussion about the P-S mass function we argued that there was a problem with considering regions of space that might be underdense on small scales but embedded in a larger overdensity. This is tricky to handle in the P-S theory because it does not explicitly link different scales. Here we will instead look at how the density field changes as we smooth it on different scales and use this to relate the behaviour of one mass to another mass through the smoothing length.

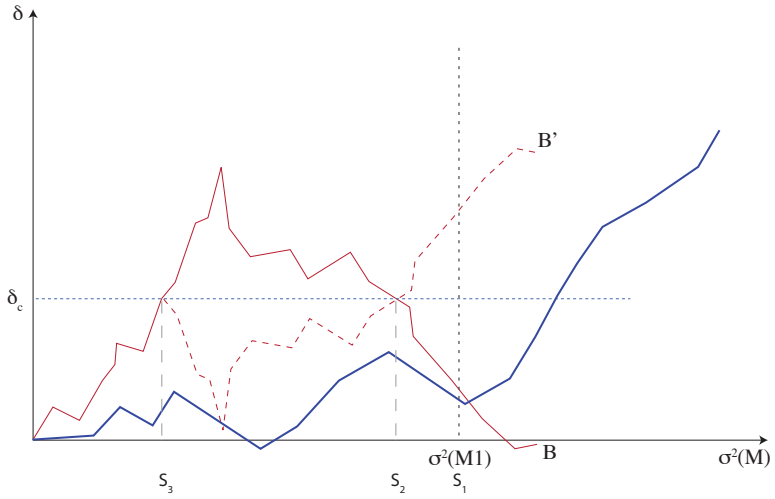

Figure 1: Illustrating the collapse of a density field on different scales. The y-axis shows the evolution of the overdensity at a given position as the smoothing scale (mass) of the density field changes along the x-axis. The region denoted B reaches an overdensity sufficient for collapse at $\sigma(M_3)^2 = S_3$ and is thus identified with a mass of M_3. B' is a reflection of this track around the line δ_c. A is a track for a region that has its first up-crossing at a $M < M_1$, or equivalently $S > S_1$.

Figure 1 shows the evolution of the overdensity of three regions of space, A, B and B', as the variance in a given window, $S = \sigma^2(M)$, increases. This corresponds to a decreasing mass. So at the left end of the plot we smooth over the entire Universe and by definition the overdensity must go to zero. As the smoothing radius decreases δ will follow a random path. In the case of a sharp k-space filter each step will be independent of the preceding step.

We identify a region as having collapsed if the overdensity is $> \delta_c$, this is marked by the horizontal dashed line in the Figure. Starting from the left, the first crossing of $\delta = \delta_c$ idenfies an object of a given mass, M, and it is the largest object that that region can be part of. We refer to this crossing as the *first up-crossing*.

If we now look at the track labelled **B** in Figure 1, we see that it crossed the $\delta = \delta_c$ line at $S = S_3 = \sigma^2(M_3)$, thus we say it is part of a structure with mass $M = M_3$. In contrast, the track **B'** took an exactly opposite step at $S = S_3$ and is obtained by reflecting the path of B for $S > S_3$ around $\delta = \delta_c$. The likelihood of B is exactly the same as for that of B', but at $S = S_1$, only B' would be counted as having a mass $M > M_1$ in the standard PS formalism. The failure to count tracks like B is the origin of the fudge factor of 2 in the Press-Schechter derivation.

Instead, in the extended PS approach, it is found to be easier to foucs on those paths, like **A**, that have their first up-crossing at $S > S_1$. In other words, these are regions that *not* part of a larger structure. In Figure 1 only track A fulfils that criterion for masses $M < M_1$, while A and B' satisfy the criterion for $M < M_3$.

Thus we want to calculate $F(M < M_1)$ which can be written as follows. To calculate this we need to start with the likelihood distribution of δ_S, ie. the density smoothed on a scale S:

$$\delta_S(\vec{x}; t) = \int \delta(\vec{x}'; t) W(\vec{x} - \vec{x}') d\vec{x}. \tag{4}$$

This likelihood we know is a Gaussian so we can write

$$P(\delta_S; M)\ d\delta_S = \frac{1}{\sqrt{2\pi}\sigma(M)} e^{-\delta_S^2/(2\sigma^2(M))}\ d\delta_S. \tag{5}$$

What then is the fraction of trajectories that have their *first* up-crossing at $S > S_1$, or equivalently $M < M_1$? Symbolically we can write:

$$\begin{aligned} F(M < M_1) = {} & \text{Fraction of tracks that have } \delta(S_1) < \delta_c - \\ & \text{Fraction of tracks that have } \delta(S_1) < \delta_c \text{ but} \\ & \text{had } \delta(S_2) > \delta_c \text{ for some } S_2 < S_1. \end{aligned}$$

Referring back to Figure 1 we want to count all tracks like A, but just making a cut of δ_S would also include tracks like B. So we need to remove those.

How do you do that? Well, for each track B, we have another track B' which has $\delta(S_1) > \delta_c$ so we calculate the fraction of tracks that satisfy this criterion and subtract it off.

We get the fractions by using the likelihood distributions for δ so for the fraction of all tracks with $\delta < \delta_c$ we have:

$$F(\delta(S_1) < \delta_c) = \int_{-\infty}^{\delta_c} P(\delta_S, M_1) d\delta_S. \tag{6}$$

That then includes also contributions from tracks like B. So we need the fraction of tracks like B' which is simply the fraction of tracks that have $\delta(S_1) > \delta_c$.

$$F(\delta(S_1) > \delta_c) = \int_{\delta_c}^{\infty} P(\delta_S, M_1) d\delta_S. \tag{7}$$

and our wanted fraction is simply the difference of these two:

$$\begin{aligned} F(M < M_1) &= F(\delta(S_1) < \delta_c) - F(\delta(S_1) > \delta_c) \\ &= \text{erf}\left[\frac{\delta_c}{\sqrt{2}\sigma(M_1)}\right], \end{aligned} \tag{8}$$

which is the result we previous found for the Press-Schechter mass function, now including the factor of 2.

3 Using the extended Press-Schechter formalism

The big advantage of the approach outlined in the preceding section is that it allows us to look at the density field at different times and scales. Thus we can start to ask very interesting questions like:

What is the probability that a collapsed halo of mass M_1 at time t_1 end up in a collapsed halo of mass M_0 at time t_0.

The two criteria there can then be summarised as:

$$\text{Collapsed halo at } t = t_1 \text{ with } M = M_1\text{:} \quad \delta(S_1) = \delta_1 = \delta_c(t_1) \tag{9}$$

where δ_1 is the value of $\delta(\vec{x})$ smoothed on a scale corresponding to mass M_1, and where $\delta_c(t)$ is given in equation (48).

The second criterion can then be written

$$\text{Collapsed halo at } t = t_0 \text{ with } M = M_0\text{:} \quad \delta(S_0) = \delta_1 = \delta_c(t_0), \tag{10}$$

These considerations are illustrated in Figure 2 where track A shows the path of a perturbation that does satisfy our criterion, while track B does not.

The key now is to realise that in previous section we were looking at changes in δ relative to $\delta = 0$, but this time we are looking at changes relative to $\delta = \delta_c(t_0)$. This

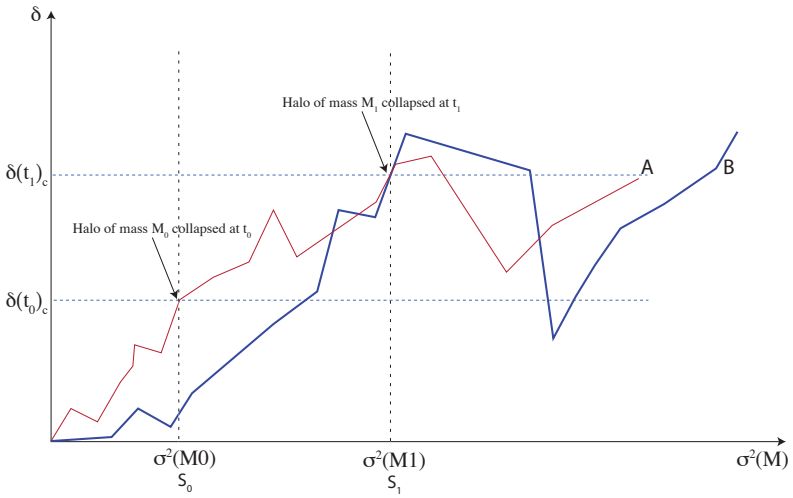

Figure 2: Like the preceding illustration, but this illustrates one track (A) of a halo that has $M = M_1$ at time t_1 and that ends up in a halo with $M = M_0$ at time t_0 where $t_0 > t_1$. While track B is for a halo that has $M = M_1$ at time t_1 but which is not part of a halo with mass M_0 at $t = t_0$.

means that the analysis is identical to that which went before except that we shift the y-axis by $\delta_c(t_0)$.

Thus we now know how to calculate

$$f_{FU}\left(M_1, \delta_c(t_1)|M_0, \delta(t_0)\right). \tag{11}$$

This function is the fraction of all halos with $M = M_1$ that collapse at time $t = t_1$ that form part of an object with mass $M = M_0$ with time $t = t_0$. Or more accurately it gives the fraction that a halo that had its first up-crossing of $\delta = \delta_c(t_1)$ at $M = M_1$, given that it has its first up-crossing of $\delta = \delta_c(t_0)$ at $M = M_0$.

We can then write this as:

$$\begin{aligned} f_{FU}\left(M_1, \delta_c(t_1)|M_0, \delta(t_0)\right) d\sigma^2(M_1) = \frac{1}{\sqrt{2\pi}} \frac{\delta_c(t_1) - \delta_c(t_0)}{(\sigma^2(M_1) - \sigma^2(M_0))^{3/2}} \times \\ \exp\left[-\frac{(\delta_c(t_1) - \delta_c(t_0))^2}{2(\sigma^2(M_1) - \sigma^2(M_0))}\right] d\sigma^2(M_1), \end{aligned} \tag{12}$$

but this looks a lot better if we define

$$\delta_1 = \delta_c(t_1) \qquad S_1 = \sigma^2(M_1) \tag{13}$$

$$\delta_0 = \delta_c(t_0) \qquad S_0 = \sigma^2(M_0) \tag{14}$$

which then turns equation (28) into

$$f_{FU}\left(M_1, \delta_1 | M_0, \delta_0\right) dS_1 = \frac{1}{\sqrt{2\pi}} \frac{\delta_1 - \delta_0}{(S_1 - S_0)^{3/2}} \exp\left[-\frac{(\delta_1 - \delta_0)^2}{2(S_1 - S_0)}\right] dS_1 \tag{15}$$

From equation (19) we can then calculate the number function. Note that this is not the number *density* function like what we calculated for the Press-Schechter mass function.

To get this we need to multiply $f_{FU}\left(M_1, \delta_1 | M_0, \delta_0\right)$ by the maximum number of M_1 halos that go into M_0, M_0/M_1:

$$N(M_1, t_1 | M_0, t_0) dM_1 = \frac{M_0}{M_1} f_{FU}\left(M_1, \delta_1 | M_0, \delta_0\right) \left|\frac{dS_1}{dM_1}\right| dM_1. \tag{16}$$

On the basis of this we can then construct mass assembly tress, so-called merger trees. This is illustrated in Figure 3, which shows a merger tree illustration from Lacey & Cole (1993). The width of the trunk reflects the mass of the halo at that time, while the branches shows merging of sub-halos to form larger halos. Such merger trees can be created using equation (20) although some care must be taken in actually implementing them on the computer.

It is useful also to define some nomenclature: We refer to the objects formed with mass M in the preceding analysis as **dark matter halos**. We refer to those halos that have merged to form a given halo as the **progenitors** of that halo.

4 Virial relations

We spent a significant time until now focusing on dark matter. Why is this? The main reason is that as we have seen in previous lectures that dark matter regulate the gravitational collapse of structures. Since dark matter perturbations can start growing as soon as the Universe becomes matter dominated, they act as seeds for the subsequent growth of baryonic structures. We saw earlier that after decoupling, baryons quickly fall into the potential wells created by the dark matter.

The collapse of dark matter leads to virialization and as I mentioned earlier and as you have shown in a problem set, in an Einstein-de Sitter Universe after the virialization of a spherical perturbation we have

$$\rho_{\rm collapse} = 18\pi^2 \bar{\rho} \equiv \Delta_c \bar{\rho} \qquad\qquad \delta_{\rm lin} = 1.69, \tag{17}$$

where $\bar{\rho}$ is the mean density of the surrounding Universe, $\delta_{\rm lin}$ is the overdensity the perturbation would have if linear theory was valid until collapse.

$\delta_{\rm lin} = 1.69$ holds true for general cosmologies to a high degree of accuracy. What about Δ_c?

The first question is perhaps whether $\bar{\rho}$ should be the critical density or the mean density of the Universe because the two co-incide for an E-dS Universe. Here we will use the generally adopted convention of referring Δ_c relative to the mean density, so that

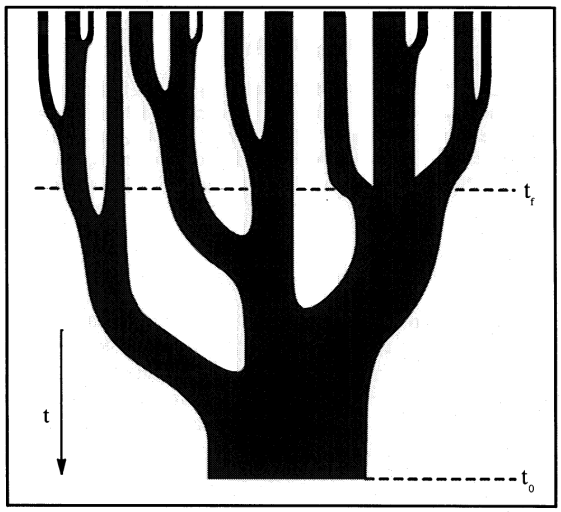

Figure 3: An illustration of a merger tree from Lacey & Cole (1993). The width of the trunk is proportional to the mass of the halo and time goes backward upwards in the picture. It is a schematic illustration of the assembly history of dark matter halos and a quantitative realisation of this can be assembled using the equations derived in the text.

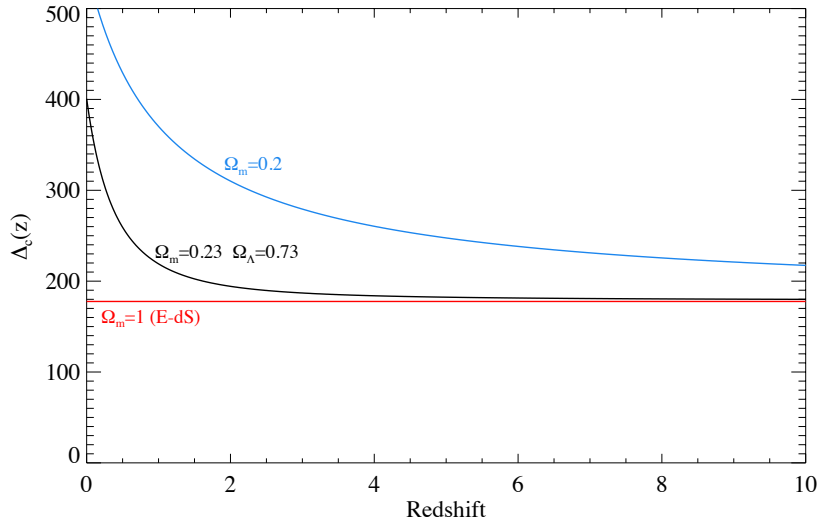

Figure 4: The change of Δ_c with redshift in three different cosmological models.

$\bar{\rho} = \Omega_m \rho_{\rm crit}$. But be aware that in the literature Δ_c is indeed sometimes given relative to the critical density — watch out for this!

At high redshift Δ_c must approach $18\pi^2$ because we have seen in the problem set that all models approach an E-dS model at sufficiently high redshift. At somewhat lower redshift it depends on the cosmological model how well $\Delta_c = 18\pi^2$ approximates the truth. Figure 4 shows the behaviour of Δ_c with redshift in three models, using the fitting formulae provided by Bryan & Norman (1998, ApJ, 495, 80). As you can see, $\Delta_c \approx 18\pi^2$ is a good approximation for flat models at $z > 2$. This means that for our needs we can use $\Delta_c = 18\pi^2$ in most cases.

This then gets us to a virialised dark matter halo. What we are interested in now is what the characteristics are of the matter within these halos. This leads us to a very useful set of relations, derived from the virial theorem and which allows us to estimate a range of physical quantities.

Below we will make use of the virial theorem repeatedly. It is therefore useful to recall the form of the virial theorem:

$$\frac{1}{2}\frac{d^2 I}{dt^2} = 2K + W + \Sigma, \tag{18}$$

where I is the moment of inertia of the system, K the kinetic energy, W the potential energy and Σ any surface terms, normally external pressure.

It is common, though not always appropriate, to assume that d^2I/dt^2 is zero or negligible. The other terms can be summarised as (we focus on the gas component here):

K: The energy per particle for a monatomic ideal gas is given by

$$\epsilon = \frac{1}{2}\mu m_P \langle v \rangle^2 = \frac{3}{2} k_B T. \tag{19}$$

If we make use of this we can then write for the total kinetic energy

$$K = \frac{3}{2}\frac{k_B T M_{\rm gas}}{\mu m_P}, \tag{20}$$

where $M_{\rm gas}$ is the mass of gas in the system.

W: The potential energy of the gas component can be written as

$$W = f_S \frac{G M M_{\rm gas}}{r_{\rm vir}}, \tag{21}$$

where f_S depends on the structure of the cloud. It is common to assume a uniform cloud in which case $f_S = 3/5$.

Σ: In the case of a significant external pressure, we can write

$$\Sigma = P_{\rm ext} 4\pi r_{\rm vir}^3, \tag{22}$$

but we often ignore this contribution. Just as we have ignored the contribution of magnetic fields (expected to be minor on galaxy scales) and turbulent pressure support.

Note that throughout the various virial relations are generally given in physical, not co-moving, coordinates.

4.1 The virial radius

The spherical collapse model has led us to write the criterion for collapse at redshift z as

$$\rho(z) \gtrsim \Delta_c \bar{\rho}(z). \tag{23}$$

If we denote the radius of the virialised region as $r_{\rm vir}$, and recall that the critical density is $\rho_{\rm crit} = 3H(z)^2/8\pi G$, we can write this criterion as

$$\rho(z) \quad \frac{1}{\bar{\rho}(z)} \qquad \gtrsim \Delta_c \tag{24}$$

$$\frac{3M}{4\pi r_{\rm vir}^3} \quad \frac{8\pi G}{\Omega_m 3H(z)^2} \gtrsim \Delta_c \tag{25}$$

During the epoch of matter domination, we can in general write $H^2(z) \approx H_0^2(1+z)^3\Omega_m$. In that case we get an expression for the virial radius

$$r_{\rm vir} = \left(\frac{2G}{H_0^2\Delta_c}\right)^{1/3} M^{1/3}(1+z)^{-1}\Omega_m^{-2/3}. \tag{26}$$

To get an idea for the order of magnitude we will here and in the following give a quantitative estimate of this referred to a halo with mass $M = 10^{12}h^{-1}M_\odot$ at $z = 0$, similar to the Milky Way; and to one at $z = 10$ with mass $M = 10^8 h^{-1}M_\odot$. Inserting values we have

$$r_{\rm vir} \approx 378 \left(\frac{M}{10^{12}h^{-1}M_\odot}\right)^{1/3} \left(\frac{\Omega_m}{0.3}\right)^{-2/3} (1+z)^{-1}h^{-1}{\rm kpc} \tag{27}$$

for the MW-like structure, while in the other case we have

$$r_{\rm vir} \approx 1.6 \left(\frac{M}{10^{8}h^{-1}M_\odot}\right)^{1/3} \left(\frac{\Omega_m}{0.3}\right)^{-2/3} \left(\frac{1+z}{11}\right)^{-1} h^{-1}{\rm kpc} \tag{28}$$

The sun is at $\sim$ 8kpc and the MW halo is $\sim 10^{12}M_\odot$ so we can conclude that the virial radius of the dark matter halo is considerably larger than that of the baryonic component. This is reasonable because baryons can release energy through radiation and hence can collapse further.

I have tacitly assumed that Δ_c is the collapse threshold derived from the spherical collapse model to get the numerical expressions above. Is this right? Well, equation 24 can be taken to define a characteristic size for the halo independently of the spherical collapse model. It is important when you come across virial radii in papers that you check what definition was used because there is no universally agreed upon definition.

4.2 The virial temperature

If we write down the virial theorem in Equation (18) ignoring external pressure and the d^2I/dt^2 term, we have

$$\frac{3M_{\rm gas}k_BT_{\rm vir}}{\mu m_P} - f_S\frac{GM_{\rm gas}M}{r_{\rm vir}} = 0, \tag{29}$$

which defines the virial temperature $T_{\rm vir}$. For a uniform sphere we have

$$T_{\rm vir} = \frac{1}{5}\frac{GM\mu m_P}{r_{\rm vir}k_B}. \tag{30}$$

It is also here common to introduce the virial velocity and in terms of this we have

$$T_{\rm vir} = \frac{1}{5}\frac{\mu m_P}{k_B}V_c^2. \tag{31}$$

If we insert $r_{\rm vir}$ from equation (26) we get

$$T_{\rm vir} = \frac{(GM)^{2/3}\mu m_P}{2^{1/3}5k_B}\Omega_m^{2/3}(1+z)H_0^{2/3}\Delta_c^{1/3}, \tag{32}$$

which gives

$$T_{\rm vir} = 1.6\times10^5\left(\frac{M}{10^{12}h^{-1}M_\odot}\right)^{2/3}\left(\frac{\Omega_m}{0.3}\right)^{2/3}\left(\frac{\mu}{0.59}\right)(1+z)K, \tag{33}$$

and

$$T_{\rm vir} = 3.9\times10^3\left(\frac{M}{10^{8}h^{-1}M_\odot}\right)^{2/3}\left(\frac{\Omega_m}{0.3}\right)^{2/3}\left(\frac{\mu}{0.59}\right)\left(\frac{1+z}{11}\right)K, \tag{34}$$

Thus we see that unless significant cooling has taken place, our galaxy is embedded in a hot halo. We will see next time how cooling influences this.

While the derivation of the virial temperature (spherical collapse, virial equilibrium, no cooling) are all very simplistic, the virial theorem remains a useful concept. Upon mergers of dark matter halos we expect in general that the gas within them gets heated to the virial temperature of the new halo, and subsequent cooling is required for star formation to start.

4.3 The circular velocity

We have made use of the circular velocity repeatedly above. This is a handy way to specify the properties of a halo because it encapsulates both the radius and mass, and for a virialised structure we can write

$$V_c = \left(\frac{GM}{r_{\rm vir}}\right)^{1/2} \tag{35}$$

$$= \left(\frac{G^2H_0^2}{2}\right)^{1/6}\Delta_c^{1/6}\Omega_m^{1/3}M^{1/3}(1+z)^{1/2}. \tag{36}$$

which shows that the circular velocity increases with mass, and also with formation redshift. Thus for the same mass and rotational velocity, the objects are more compact at high redshift.

Quantitatively this results for our examples in:

$$V_c = 107 \left(\frac{M}{10^{12} h^{-1} M_\odot}\right)^{1/3} (1+z)^{1/2} \left(\frac{\Omega_m}{0.3}\right)^{1/3} \text{km/s} \tag{37}$$

$$= 16 \left(\frac{M}{10^{8} h^{-1} M_\odot}\right)^{1/3} \left(\frac{1+z}{11}\right)^{1/2} \left(\frac{\Omega_m}{0.3}\right)^{1/3} \text{km/s} \tag{38}$$

The Milky Way has a circular velocity of $V_c \approx 220$km/s which is somewhat higher than what you expect from the above scalings. A possible interpretation is that the halo of the Milky Way virialised at $z \sim 3$, but recall that this is a very simplistic model.

5 The structure of dark matter halos

See section 5.2.1 in MvdBW for a discussion of the self-similar spherical collapse model. Section 7.5 in the same book discusses the internal structure of dark matter halos.

It is possible to show, but cumbersome, that in a spherical collapse model with self-similar solutions the density profile of the resulting dark matter halo can be expected to be a power-law, and one can argue from this that typical dark matter halos should have density profiles that are close to isothermal,

$$\rho_{isothermal} \propto r^{-2}. \tag{39}$$

This is a handy profile from an analytic point of view and it is useful to tabulate some classical relationships for this profile.

$$\rho(r) = \frac{2k_B T}{\mu m_P} \frac{1}{4\pi G r^2} \tag{40}$$

$$M(r) = \frac{2k_B T}{\mu m_P} \frac{r}{G}, \tag{41}$$

but it is also common to see these relations phrased in terms of the circular velocity, $V_c = \sqrt{GM/r}$, which gives:

$$V_c^2 = \frac{2k_B T}{\mu m_P} \tag{42}$$

$$\rho(r) = \frac{V_c^2}{4\pi G r^2} \tag{43}$$

$$M(r) = \frac{V_c^2 r}{G}. \tag{44}$$

Since this profile does not have a convergent mass, it is common to truncate this at the virial radius, creating the truncated isothermal sphere.

Simulations of dark matter halos do however show that their profiles are not isothermal spheres. Notably, however, simulations *do* show that dark matter profiles have a universal shape. This was noticed by Navarro, Frenk & White (1996) and their fit to this profile, the Navarro-Frenk-White (NFW) profile has become the most widely used density profile for dark matter halos.

This profile has the shape

$$\rho(r) = \bar{\rho}\frac{\delta_{\rm char}}{(r/r_s)(1+r/r_s)^2}, \tag{45}$$

with mass

$$M(<r) = 4\pi\bar{\rho}\delta_{\rm char}r_s^3\left[\ln(1+cx) - \frac{cx}{1+cx}\right], \tag{46}$$

where $c = r_{\rm vir}/r_s$, $x = r/r_{\rm vir}$ and if you combine this with the criterion for top-hat collapse which we reviewed above, you can show that

$$\delta_{\rm char} = \frac{\Delta_c}{3}\frac{c^3}{\ln(1+c) - c/(1+c)}. \tag{47}$$

The parameter c is known as the concentration parameter and from equation (47) one can see that M and c is sufficient to specify the shape of the halo. It is known that c is a function of halo mass and formation time and fits have been provided in the literature for this dependence.

The fact that mass profiles to first order depend only on the halo mass is an important observation, and one that we will make use of later.

A Ideal gas

An ideal gas is an idealised concept of identical point particles that do not interact and when they collide all collisions are elastic. However despite its simplicity it does give a fairly good description of gas behaviour in many situations in galaxy formation. The basic law for ideal gas is

$$PV = Nk_BT, \tag{48}$$

with P being the pressure, V the volume, T the temperature and N the number of gas particles; k_B is Boltzmann's constant as usual.

In astrophysics it is common to introduce the mean mass per particle in units of the proton mass, μ, so that the mass per particle is μm_P, and to use the density, ρ, instead of the number of particles. In that case equation (48) is transformed into

$$P = \frac{k_BT}{\mu m_P}\rho. \tag{49}$$

The internal energy of the gas is

$$\mathcal{E} = \frac{1}{\gamma - 1} \frac{k_B T}{\mu m_P}, \tag{50}$$

with γ the ratio of the specific heats, $\gamma = C_P/C_V$, which for an ideal gas is given as $\gamma = (q+5)/(q+3)$ with q the number of internal degrees of freedom. We will essentially only be concerned with monatomic gases for which $q = 0$ and hence $\gamma = 5/3$.

The mean mass per particle in units of the proton mass, μ, is an important ingredient in many of the expressions we will use in the following. It is therefore useful to recall how to calculate μ in different scenarios. By definition we have

$$m_P \mu = \frac{m_{\rm tot}}{N_{\rm tot}}. \tag{51}$$

If we introduce the mass fraction of hydrogen, $X = m_H/m_{\rm tot}$, and that of helium, $Y = m_{\rm He}/m_{\rm tot}$, we can express μ in terms of Y for different scenarios. The two main scenarios for us a complete neutral gas and a fully ionized gas.

For a neutral gas we have

$$N_{\rm tot} = N_{\rm H} + N_{\rm He} = \left(X + \frac{Y}{4} \right) \frac{m_{\rm tot}}{m_P}, \tag{52}$$

so you get

$$\mu_{\rm neutral} = \frac{4}{4 - 3Y} = \frac{16}{13} \approx 1.23. \tag{53}$$

In a fully ionised gas we have

$$\mu = \frac{16}{27} \approx 0.59. \tag{54}$$

It is also useful to use these results to relate the electron density and hydrogen densities to each other and to the total number density, since the expressions above are equally valid when formulated in terms of number densities I write the following equalities for number densities and for a fully ionised gas we have:

$$n_e = n_{\rm H} + 2n_{\rm He} = \frac{7}{6} n_{\rm H} \tag{55}$$

$$n_e = \frac{14}{27} n_{\rm tot} \tag{56}$$

$$n_{\rm H} = \frac{4}{9} n_{\rm tot} \tag{57}$$